

Single-component Layered Molecular Conductor, [Au(ptdt)₂]Biao Zhou,¹ Hiroyuki Yajima,¹ Yuki Idobata,¹ Akiko Kobayashi,*¹ Tetsuya Kobayashi,²
Eiji Nishibori,² Hiroshi Sawa,² and Hayao Kobayashi¹¹Department of Chemistry, College of Humanities and Sciences, Nihon University,
3-25-40 Sakurajosui, Setagaya-ku, Tokyo 156-8550²Department of Applied Physics, Nagoya University, Nagoya, Aichi 464-8603

(Received October 29, 2011; CL-111058; E-mail: akoba@chs.nihon-u.ac.jp)

A single-component layered molecular conductor, [Au(ptdt)₂] (ptdt: propylenedithiotetrafulvalenedithiolate) was prepared. Unlike the single-component molecular metal, [Au(tmdt)₂] (tmdt: trimethylenetetrafulvalenedithiolate) exhibiting three-dimensional compact molecular packing and antiferromagnetic transition at 110 K, the compressed pellet of the microcrystals of [Au(ptdt)₂] exhibited fairly high conductivity and small temperature-independent paramagnetic susceptibility.

In 1999, the crystal structure and electrical properties of a single-component molecular conductor, [Ni(ptdt)₂] (Chart 1), were reported.¹ Although [Ni(ptdt)₂] did not exhibit metallic properties, it exhibited high conductivity. This high conductivity of the crystal convinced us of the validity of our idea regarding the design of a single-component molecular metal.² Two years later, the first single-component molecular metal, [Ni(tmdt)₂], was realized by using an analogous extended-TTF-type (TTF: tetrathiafulvalene) dithiolate ligand, tmdt.³ The observation of de Haas-van Alphen oscillations at very high magnetic fields and low temperatures as well as ab initio band structure calculations proved the existence of the three-dimensional (3D) Fermi surfaces (FSs).^{4,5}

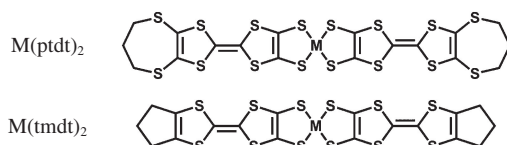


Chart 1.

To date, various single-component molecular metals including a series of isostructural [M(tmdt)₂] (M = Ni, Cu, Pd, Au, and Pt) systems have been reported.⁶ The high controllability of the electronic band structure achieved by exchanging the central metal atom (M) for another transition metal is an important characteristic of the single-component molecular conductor. The electronic band structure of [M(tmdt)₂] near the Fermi level is determined mainly by three molecular orbitals, namely, *sym-Lπ*, *asym-Lπ(d)*, and *pdσ(-)* orbitals (Figure 1).⁸ The *sym-Lπ* and *asym-Lπ(d)* orbitals form 3D stable metal bands in the Ni, Pd, and Pt complexes with an even number of total electrons. On the other hand, the *asym-Lπ(d)* orbital becomes the singly occupied molecular orbital (SOMO) of Au(tmdt)₂ with an odd number of total electrons, and [Au(tmdt)₂] becomes a magnetic metal exhibiting antiferromagnetic transition at 110 K (in this paper, [M(tmdt)₂] and M(tmdt)₂ represent the crystal of a single-

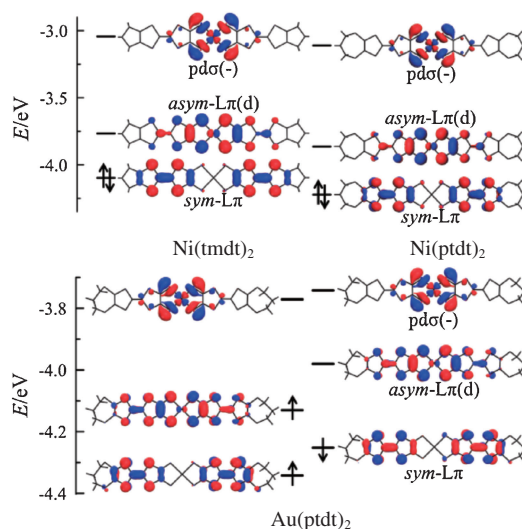


Figure 1. Nonspin-polarized molecular orbitals (MOs) of Ni(tmdt)₂ and Ni(ptdt)₂ and spin-polarized MOs of Au(ptdt)₂.⁷

component molecular conductor and the constituent molecule, respectively).⁹ In the case of [Cu(tmdt)₂], *pdσ(-)* becomes the SOMO and an antiferromagnetic chain coexists with π conduction electrons.¹⁰

In addition to the frontier molecular orbital properties, the mode of molecular arrangement, which is controllable to a certain extent by the type of ligand (L) used, plays a crucial role in the determination of the band structure of a single-component molecular conductor [M(L)₂]. A variety of electronic structures can be realized by using different combinations of M and L. However, the role of L, especially the bulkiness of the terminal alkyl group of L has not been investigated sufficiently. In this work, [Au(ptdt)₂] was prepared in order to study the effect of the terminal alkyl group on the band structure and electromagnetic properties of single-component molecular conductor.

All the syntheses were carried out under a strictly inert atmosphere. The ptdt ligand was synthesized according to a procedure described in the literature.¹¹ The deprotection of the ptdt ligand using a MeOH solution of tetramethylammonium hydroxide in dry THF at room temperature yielded reddish-orange precipitates of (Me₄N⁺)₂(ptdt²⁻). After cooling to -78 °C, the THF solution of (*n*-Bu₄N)[AuCl₄] was added to the system. Dark green-colored complexes of (Me₄N)[Au(ptdt)₂] were obtained. The crystals of neutral [Au(ptdt)₂] were prepared electrochemically using an H-shaped cell containing *n*-Bu₄N·PF₆ dissolved in acetonitrile. After applying a current of 0.4 μ A for 4 weeks, black needle microcrystals were obtained. X-ray

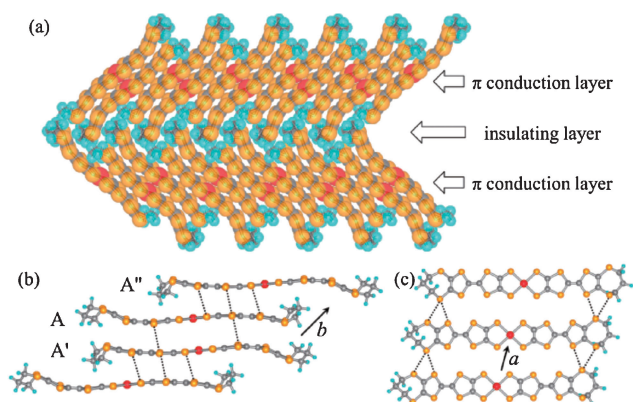


Figure 2. (a) Molecular packing in $[\text{Au}(\text{ptdt})_2]$. Yellow, gray, and sky blue spheres represent S, C, and H atoms, respectively. (b) The molecular arrangement along the b axis. (c) The molecular arrangement along the a axis, where the short intermolecular S...S contacts are shown as dotted lines.

powder diffraction experiments were performed at the BL02B2 in the SPring-8 facility of the Japan Synchrotron Radiation Research Institute. The crystal structure was determined by a modified genetic algorithm (GA) and refined by the MEM/Rietveld method.¹²

We found that $[\text{Au}(\text{ptdt})_2]$ is not isostructural to $[\text{Ni}(\text{ptdt})_2]$.¹ It has been considered that unlike conventional organic conductors consisting of π conduction layers and insulating anion layers, single-component molecular conductors tend to have 3D stable metallic bands. A typical example is $[\text{Pt}(\text{tmdt})_2]$, which exhibits metallic behavior down to liquid helium temperature even in the form of a compressed pellet of microcrystals.¹³ However, in the case of $[\text{Au}(\text{ptdt})_2]$, the bulky terminal group of the ptdt ligands inhibits the formation of 3D compact molecular packing, and the crystal of $[\text{Au}(\text{ptdt})_2]$ has a 2D layered structure (Figure 2a). $\text{Au}(\text{ptdt})_2$ molecules are stacked along the b axis and arranged side-by-side along the a axis to form a conduction layer parallel to the ab plane. There is no short S...S contact between adjacent layers. In addition, as shown in Figure 1, the frontier molecular orbitals ($\text{sym-L}\pi$ and $\text{asym-L}\pi(\text{d})$) of $\text{Au}(\text{ptdt})_2$ possess almost no amplitude on the outermost S atoms. Consequently, the interlayer interactions will become very small to make the system 2D conductor. A similar 2D structure has also been observed in single-component molecular conductors with bulky ligands, such as $[\text{Ni}(\text{ptdt})_2]$ and $[\text{M}(\text{hfdt})_2]$ ($\text{M} = \text{Ni}$ and Au ; hfdt: bis(trifluoromethyl)tetrathiafulvalene).^{1,14} A gold atom has a square-planar coordination with an average Au–S distance of 2.265 Å and an S–Au–S angle of 88.10°; these values are approximately equal to the bond length and the angle found in $\text{Au}(\text{tmdt})_2$ (2.300 Å and 89.11°), respectively.⁹ The shortest intermolecular S...S distance is 3.263 Å along the a axis (Figure 2c). Those between molecules A and A' and molecules A and A'' are 3.573 and 3.452 Å, respectively (Figure 2b).

The electronic band structure calculations were performed by using a periodic density functional plane wave code using CASTEP software (Materials Studio, Accelrys).⁷ The MOs of $\text{Au}(\text{ptdt})_2$ are shown in Figure 1. The calculated density of states (DOS), FSs, and band energy dispersion curve of $[\text{Au}(\text{ptdt})_2]$ are shown in Figure 3. The band dispersion was very small along

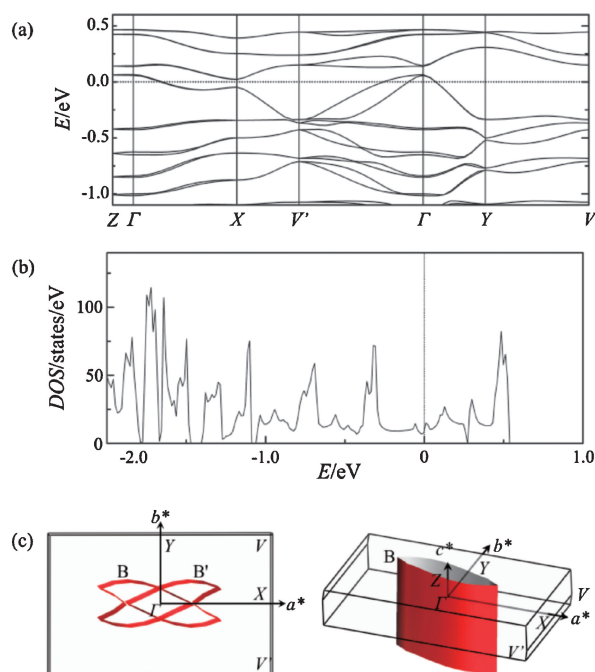


Figure 3. The results of density functional theory (DFT) band structure calculations of $[\text{Au}(\text{ptdt})_2]$. (a) Band energy dispersion curve, (b) DOS, and (c) Fermi surfaces of $[\text{Au}(\text{ptdt})_2]$. B and B' correspond to the Fermi surfaces of neighboring two layers with different orientations. 2D Fermi surface of one conduction layer (B) are also presented, where small interlayer interactions are neglected.

the c^* direction, and flattened cylindrical 2D FSs was obtained. The examination of the band structures of the hitherto-reported single-component molecular conductors consisting of the molecules with bulky ligands such as ptdt and hfdt suggested that FSs are barely observed in these conductors. Owing to the crossing-band nature of $[\text{Ni}(\text{ptdt})_2]$, FS of this system was thought to be very small even if it exists.¹ In addition, $[\text{M}(\text{hfdt})_2]$ ($\text{M} = \text{Ni}$ and Au) has no FS due to the energy gap at Fermi energy (ε_{F}).¹⁴ On the other hand, the simple band dispersion near ε_{F} suggested that 2D FSs will certainly exist in $[\text{Au}(\text{ptdt})_2]$ (Figure 3a).

Resistivity measurements were performed on the compressed pellets of microcrystals of $[\text{Au}(\text{ptdt})_2]$ at temperatures in the range of 4.2–300 K (Figure 4). The room-temperature conductivity ($\sigma_{\text{RT}} \approx 2 \text{ S cm}^{-1}$) was fairly high for a compressed pellet sample of a 2D molecular conductor. In addition, the activation energies of the resistivities were very small ($\Delta E = 18 \text{ meV}$ at 100–150 K and 28 meV at 200–300 K). These results indicated $[\text{Au}(\text{ptdt})_2]$ to be essentially metallic in the single-crystal state, as suggested from the band-structure calculations (Figure 3).

The magnetic susceptibility was measured by using a SQUID magnetometer at temperatures in the range of 2–300 K (Figure 4b). Unlike $[\text{Au}(\text{tmdt})_2]$, which exhibits antiferromagnetic transition at 110 K, $[\text{Au}(\text{ptdt})_2]$ does not exhibit any distinct magnetic anomaly. The increase in susceptibility at low temperatures is attributed to the paramagnetic ($S_{1/2}$) impurities of 1.3%. The diamagnetic contribution was estimated from Pascal's constants to be $-3.5 \times 10^{-4} \text{ emu mol}^{-1}$. At temperatures above

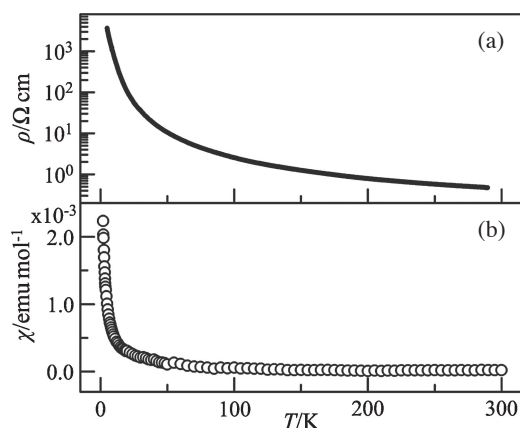


Figure 4. (a) Temperature dependences of resistivities of [Au(ptdt)₂]. (b) Temperature dependences of magnetic susceptibility.

80 K, the susceptibility was almost temperature-independent; this indicated the metallic nature of the crystal. However, the temperature-independent paramagnetic susceptibility was obtained after the subtraction of the Curie impurity susceptibility, and Pascal's diamagnetic term was approximately 1.0×10^{-5} emu mol⁻¹, which is more than one order of magnitude smaller than the standard paramagnetic susceptibility of the molecular conductor. The calculated DOS of [Au(ptdt)₂] at ε_F ($D(\varepsilon_F)$) is approximately 10 electrons/eV/unit cell (Figure 3b), and that of [Au(tmdt)₂] with a room-temperature paramagnetic susceptibility of 4.2×10^{-4} emu mol⁻¹ is reported to be approximately 8 electrons/eV/unit cell.^{8c,9b} These values and the unexpectedly low paramagnetic susceptibility of [Au(ptdt)₂] indicate the possibility that the diamagnetic correction of [Au(ptdt)₂] is much larger than that estimated from Pascal's constants. However, the origin of this discrepancy is not clear at present.

In conclusion, a new single-component molecular conductor, [Au(ptdt)₂], was prepared. Unlike typical single-component molecular metals [M(tmdt)₂] (M = Ni, Pd, Pt, and Au) with a 3D tight molecular packing, [Au(ptdt)₂] has a crystal structure with layered molecular packing. The crystals of [Au(ptdt)₂] are composed of 2D layers of Au(ptdt)₂ molecules, and the π conduction layers are separated by terminal propylenedithio groups and outermost S atoms. The DFT band structure calculations suggested that [Au(ptdt)₂] was the first single-component 2D metal with flattened cylindrical FSs. It was confirmed that the single-component molecular conductor [M(L)₂] can possess a wide variety of electronic band structures by adopting various combinations of M and L. The resistivity measurements performed on the compressed pellets of microcrystals showed fairly high room-temperature conductivity (ca. 2 S cm⁻¹) and very low activation energy. The paramagnetic susceptibility was temperature-independent, with a very low value (ca. 1.0×10^{-5} emu mol⁻¹). However, the estimation of diamagnetic susceptibility of [Au(ptdt)₂] remains to be a future problem.

This work was financially supported by Grants-in-Aid for Scientific Research (B) (No. 20350069), Young Scientists (B) (No. 21750153), and Innovative Areas (No. 20110003) from the

Ministry of Education, Culture, Sports, Science and Technology of Japan. The study was also supported by the "Strategic Research Base Development" Program for Private Universities subsidized by MEXT (2009) (No. S0901022). The synchrotron radiation experiments were performed at the BL02B2 in the SPring-8 facility with the approval from the Japan Synchrotron Radiation Research Institute (JASRI).

References and Notes

- 1 A. Kobayashi, H. Tanaka, M. Kumasaki, H. Torii, B. Narymbetov, T. Adachi, *J. Am. Chem. Soc.* **1999**, *121*, 10763.
- 2 A. Kobayashi, H. Tanaka, H. Kobayashi, *J. Mater. Chem.* **2001**, *11*, 2078.
- 3 H. Tanaka, Y. Okano, H. Kobayashi, W. Suzuki, A. Kobayashi, *Science* **2001**, *291*, 285.
- 4 H. Tanaka, M. Tokumoto, S. Ishibashi, D. Graf, E. S. Choi, J. S. Brooks, S. Yasuzuka, Y. Okano, H. Kobayashi, A. Kobayashi, *J. Am. Chem. Soc.* **2004**, *126*, 10518.
- 5 C. Rovira, J. J. Novoa, J.-L. Mozos, P. Ordejón, E. Canadell, *Phys. Rev. B* **2002**, *65*, 081104.
- 6 a) A. Kobayashi, E. Fujiwara, H. Kobayashi, *Chem. Rev.* **2004**, *104*, 5243. b) D. Belo, H. Alves, E. B. Lopes, M. T. Duarte, V. Gama, R. T. Henriques, M. Almeida, A. Pérez-Benítez, C. Rovira, J. Veciana, *Chem.—Eur. J.* **2001**, *7*, 511. c) J. P. M. Nunes, M. J. Figueira, D. Belo, I. C. Santos, B. Ribeiro, E. B. Lopes, R. T. Henriques, J. Vidal-Gancedo, J. Veciana, C. Rovira, M. Almeida, *Chem.—Eur. J.* **2007**, *13*, 9841. d) N. Tenn, N. Belleç, O. Jeannin, L. Piekara-Sady, P. Auban-Senzier, J. Íñiguez, E. Canadell, D. Lorcay, *J. Am. Chem. Soc.* **2009**, *131*, 16961.
- 7 a) CASTEP is available as part of Material Studio Modeling v5.0 software package (Accelrys Inc., San Diego, CA). b) J. P. Perdew, K. Burke, M. Ernzerhof, *Phys. Rev. Lett.* **1996**, *77*, 3865.
- 8 a) S. Ishibashi, H. Tanaka, M. Kohyama, M. Tokumoto, A. Kobayashi, H. Kobayashi, K. Terakura, *J. Phys. Soc. Jpn.* **2005**, *74*, 843. b) H. Seo, S. Ishibashi, Y. Okano, H. Kobayashi, A. Kobayashi, H. Fukuyama, K. Terakura, *J. Phys. Soc. Jpn.* **2008**, *77*, 023714. c) S. Ishibashi, K. Terakura, A. Kobayashi, *J. Phys. Soc. Jpn.* **2008**, *77*, 024702.
- 9 a) W. Suzuki, E. Fujiwara, A. Kobayashi, Y. Fujishiro, E. Nishibori, M. Takata, M. Sakata, H. Fujiwara, H. Kobayashi, *J. Am. Chem. Soc.* **2003**, *125*, 1486. b) B. Zhou, M. Shimamura, E. Fujiwara, A. Kobayashi, T. Higashi, E. Nishibori, M. Sakata, H. Cui, K. Takahashi, H. Kobayashi, *J. Am. Chem. Soc.* **2006**, *128*, 3872.
- 10 B. Zhou, H. Yajima, A. Kobayashi, Y. Okano, H. Tanaka, T. Kumashiro, E. Nishibori, H. Sawa, H. Kobayashi, *Inorg. Chem.* **2010**, *49*, 6740.
- 11 a) L. Binet, J. M. Fabre, C. Montginoul, K. B. Simonsen, J. Becher, *J. Chem. Soc., Perkin Trans. 1* **1996**, 783. b) L. Binet, C. Montginoul, J. M. Fabre, L. Ouahab, S. Golhen, J. Becher, *Synth. Met.* **1997**, *86*, 1825.
- 12 X-ray crystallographic data of [Au(ptdt)₂]: C₁₈H₁₂AuS₁₆, $M_r = 938.29$, monoclinic, space group $P2_1/n$, $a = 6.6545(1) \text{ \AA}$, $b = 10.9312(2) \text{ \AA}$, $c = 38.1670(9) \text{ \AA}$, $\beta = 92.922(15)^\circ$, $V = 2772.72 \text{ \AA}^3$, $Z = 4$, The final R_{wp} and R_1 are 2.2% and 5.4%, respectively. CCDC-851158.
- 13 B. Zhou, A. Kobayashi, Y. Okano, T. Nakashima, S. Aoyagi, E. Nishibori, M. Sakata, M. Tokumoto, H. Kobayashi, *Adv. Mater.* **2009**, *21*, 3596.
- 14 M. Sasa, E. Fujiwara, A. Kobayashi, S. Ishibashi, K. Terakura, Y. Okano, H. Fujiwara, H. Kobayashi, *J. Mater. Chem.* **2005**, *15*, 155.